Synthesis, Characterization, and Rearrangements of Methoxymethyl Ruthenium(II) Complexes with Polypyridine Ligands

Dorothy H. Gibson,* Jose G. Andino, and Mark S. Mashuta

Department of Chemistry, University of Louisville, Louisville, Kentucky 40292

Received June 3, 2005

Three stereoisomeric methoxymethyl complexes, [Ru(bpy)(η^2-tpy)(CO)CH_2OMe]PF_6 (**2a**−**c**), have been synthesized and structurally characterized. Also, the precursor complexes *cis*-[Ru(η^3-tpy)(CO)(S)CH_2OMe]PF_6 (**3**, **4**; S = MeCN, MeOH) have been synthesized and structurally characterized. Packing diagrams indicate extensive $\pi-\pi$ stacking interactions for **2a**−**2c**. Compounds **2b** and **2c** are linkage isomers, while **2a** has distinct stereochemistry; **2b** and **2c** establish equilibrium in solution and slowly convert to **2a**. Independent studies beginning with pure **2b** or **2c** did not establish whether one, or both, can isomerize to **2a**. Nondissociative trigonal twist mechanisms, in some cases followed by linkage isomerization, can rationalize the isomerizations. Alternatively, isomerization of **2b** to **2a** may occur by a "conrotatory twist" pathway followed by linkage isomerization. The compounds are models for putative intermediates in electrocatalytic reductions of CO_2.

Introduction

Ruthenium(II) complexes with polypyridine ligands have been studied for many years as electrocatalysts for the reduction of carbon dioxide.[1] In most cases, the reduction products have been CO and/or formate. A number of years ago, Tanaka and co-workers[2] reported that the use of [Ru(bpy)(tpy)(CO)]$2PF_6$ (bpy = 2,2′-bipyridine, tpy = 2,2′:6′,2″-terpyridine) as an electrocatalyst for CO_2 reduction afforded C_2 products, glyoxylic acid and glycolic acid, in addition to formaldehyde, formic acid, and methanol. Significantly, the C_2 products were obtained only from reactions conducted at −20 °C; catalytic reactions conducted at room temperature did not produce the C_2 compounds. Also, reactions conducted with a related cation, [Ru$(bpy)_2(CO)_2$]$2PF_6$, did not produce C_2 compounds under any conditions. The catalytic pathways for the C_2 products were not established, and since the reductions were both unusual and important observations, we began work on some organometallic complexes with C_1 ligands that seemed to be plausible intermediates. Of particular interest were formyl and hydroxymethyl complexes which might be generated as the result of reverse water gas shift (WGS) reactions that could take place under the catalytic conditons followed by catalytic reductions of cations with the general formula [Ru(bpy)(η^2-tpy)$(CO)_2$]$2PF_6$; there are two such isomeric cations.[3] The sequence shown in Scheme 1 represents a possible pathway from a formyl complex, **1a** (see Chart 1), that can be derived from one of these cations to glyoxylic acid. Migratory insertion involving an acyl (but not formyl) group is known,[4] and there is recent precedent for migratory insertion driven by the pendant pyridine group of an η^2-terpyridine ligand.[5] Hydrolytic cleavage of an acyl group is also known.[6]

Scheme 1

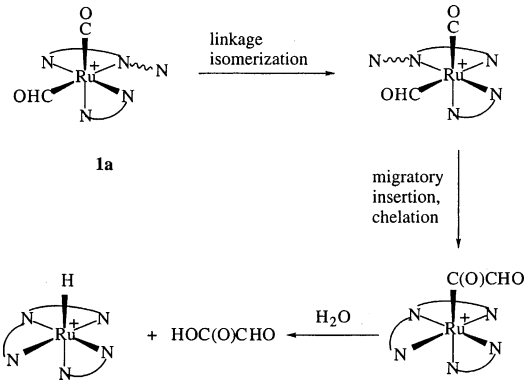

(1) (a) Hawecker, J.; Lehn, J. M.; Ziessel, R. *J. Chem. Soc., Chem. Commun.* **1983**, 536. (b) Sullivan, B. P.; Bolinger, C. M.; Conrad, D.; Vining, T. J.; Meyer, T. J. *J. Chem. Soc., Chem. Commun.* **1985**, 1414. (c) Sullivan, B. P.; Conrad, D.; Meyer, T. J. *Inorg. Chem.* **1985**, *24*, 3640. (d) Hawecker, J.; Lehn, J.-M.; Ziessel, R. *Helv. Chim. Acta* **1986**, *69*, 1990. (e) Ishida, H.; Tanaka, K.; Tanaka, T. *Organometallics* **1987**, *6*, 181. (f) Bruce, M. R. M.; Megehee, E.; Sullivan, B. P.; Thorp, H.; O'Toole, T. R.; Downard, A.; Meyer, T. J. *Organometallics* **1988**, *7*, 238. (g) Sullivan, B. P.; Bruce, M. R. M.; O'Toole, T. R.; Bolinger, C. M.; Megehee, E.; Thorp, H.; Meyer, T. J. In *Catalytic Activation of Carbon Dioxide*; Ayers, W. M., Ed.; ACS Sym. Ser. 363, American Chemical Society; Washington, D.C., 1988; Chapter 6. (h) Ziessel, R. In *Catalysis by Metal Complexes: Photosensitization and Photocatalysis Using Inorganic and Organometallic Compounds*; Kalyanasundaram, K., Grätzel, M., Eds.; Kluwer Academic Publishers: Dordrecht, Netherlands, 1993; p 217. (i) Christensen, P.; Hammett, A.; Muir, A. V. G.; Timney, J. H. *J. Chem. Soc., Dalton Trans.* **1992**, 1455. (j) Yoshida, T.; Tsutsumida, K.; Teratani, S.; Yasufuku, K.; Kaneko, M. *J. Chem. Soc., Chem. Commun.* **1993**, 631. (k) Stor, G. J.; Hartl, F.; van Outersterp, J. W. M.; Stufkens, D. J. *Organometallics* **1995**, *14*, 115. (l) Johnson, F. P. A.; George, M. W.; Hartl, F.; Turner, J. J. *Organometallics* **1996**, *15*, 3374. (m) Klein, A.; Vogler, C.; Kaim, W. *Organometallics* **1996**, 15, 236. (n) Sutin, N.; Creutz, C.; Fujita, E. *Comments Inorg. Chem.* **1997**, *19*, 67. (o) Scheiring, T.; Klein, A.; Kaim, W. *J. Chem. Soc., Perkin Trans. 2* **1997**, 2569.

(2) Nagao, H.; Mizukawa, T.; Tanaka, K. *Inorg. Chem.* **1994**, *33*, 3415.

(3) Gibson, D. H.; Andino, J. G.; Bhamidi, S.; Sleadd, B. A.; Mashuta, M. S. *Organometallics* **2001**, *20*, 4956.

(4) (a) Sheridan, J. B.; Johnson, J. R.; Handwerker, B. M.; Geoffroy, G. L.; Rheingold, A. L. *Organometallics* **1988**, 7, 2404. (b) Geoffroy, G. L.; Sheridan, J. B.; Bussmer, S. L.; Kelley, C. *Pure Appl. Chem.* **1989**, *61*, 1723.

10.1021/om058031w CCC: $30.25
Publication on Web 09/15/2005

Chart 1[a]

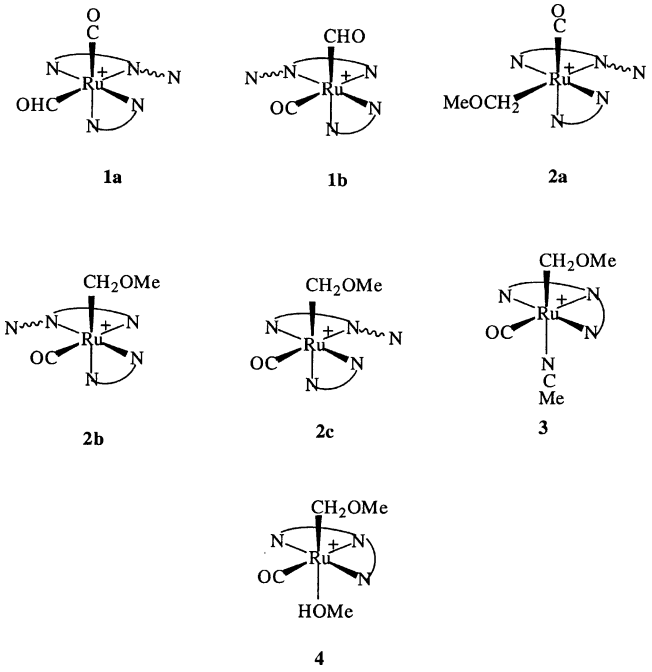

[a] N-N = 2,2′-bipyridine; N-N-N = 2,2′:6′,2″-terpyridine.

We prepared and characterized two isomeric formyl complexes [Ru(bpy)(η^2-tpy)(CO)(CHO)]PF_6 (**1a**, **1b**; see Chart 1) and the corresponding hydroxymethyl complexes.[3] As we began to study these complexes, we found that they were labile in solution. The formyl complexes degrade upon standing in solution, and the hydroxymethyl complexes lost formaldehyde readily in solution, a characteristic of such compounds.[7] As noted above, formaldehyde is one of the reduction products in the Tanaka study.[2] Also, we observed that the formyl and hydroxymethyl complexes with the stereochemistry shown for formyl complex **1b** would rearrange to the **1a**-type isomers in solution. Furthermore, an additional isomer appeared as a small component in each case, but eventually disappeared as the isomerization went to completion.[8] Because of the lability of the formyl and hydroxymethyl complexes, we sought a related C_1 derivative that might exhibit the isomerization behavior of the other two without the likelihood of rapid degradation. Compounds **2a** and **2b** (Chart 1) were targeted for study. The synthesis and unusual reactions of these compounds are described in the present study.

Results and Discussion

It was necessary to prepare and characterize both methoxymethyl complexes (**2a**, **2b**). We began with reaction of formyl complex **1a** with *p*-toluenesulfonic acid in methanol; the reaction afforded approximately equal amounts of the dicarbonyl cation and complex **2a** and proceeds according to the general eq 1. The two

$$\mathrm{M{-}CHO} + \mathrm{H^+} \xrightarrow[\mathrm{MeOH}]{} \mathrm{M{=}CHOMe^+} \xrightarrow[+\,\mathrm{M\text{-}CHO}]{-\,\mathrm{M(CO)^+}} \mathrm{M{-}CH_2OMe} \quad (1)$$

products are easily separated by solubility differences (see Experimental Section). This method had been used successfully some years ago for the conversion of cationic or neutral formyl complexes to the corresponding alkoxymethyl complexes and requires that the formyl complex be a relatively strong hydride donor.[9] Compound **2a** has been characterized by elemental analysis, ^1H and ^{13}C NMR and IR spectroscopy, and X-ray crystallography. Figure 1 shows the ORTEP diagram[10] for **2a** (cation only). The crystallographic data are shown in Table 1, and selected bond distances and bond angles are shown in Table 2. As Figure 1 shows, the stereochemistry assigned to **1a** and established for its hydroxymethyl analogue[3] is retained in **2a**. The cation shows distorted octahedral geometry about the ruthenium atom with the C(2)−Ru−N(4) bond angle deviating greatly from linearity at 166.52(11)°. The Ru−N(4) bond distance is 2.229(2) Å and is nearly one-tenth of an angstrom longer than the other Ru−N bond distances in the cation. This is likely due to the trans influence of the methoxymethyl group, which is expected to be a strong σ donor.[11] The orientation of the pendant pyridine ring suggested $\pi-\pi$ stacking, and indeed, analysis of nonbonded forces reveals a centroid-to-centroid distance between the pendant pyridine and one of the bipyridine rings (see Figures 1a and 1b in the Supporting Information for views of the packing diagram for **2a**) of 3.483 Å and is well within the 3.3−3.8 Å range for such interactions; aromatic heterocycles, such as bpy and tpy, are thought to be well-suited for

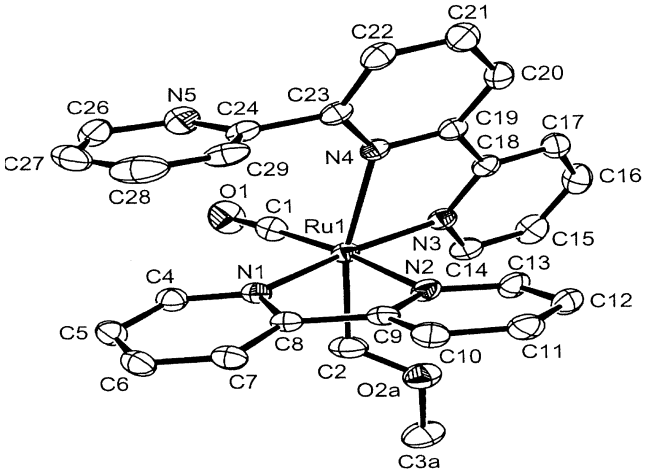

Figure 1. ORTEP drawing of **2a** (cation only) with thermal ellipsoids shown at the 50% probability level.

(5) Groen, J. H.; de Zwart, A.; Vlaar, M. J. M.; Ernsting, J. M.; van Leeuwen, P. W. N. M.; Vrieze, K.; Kooijman, H.; Smeets, W. J. J.; Spek, A. L.; Budzelaar, P. H. M.; Xiang, Q.; Thummel, R. P. *Eur. J. Inorg. Chem.* **1998**, 1129.

(6) (a) Abel, E. W.; Dimitrou, V. S.; Long, N. J.; Orrell, K. G.; Osbourne, A. G.; Sik, V.; Hursthouse, M. B.; Mazid, M. A. *J. Chem. Soc., Dalton Trans.* **1993**, 291. (b) Civetello, E. R.; Dragovitch, P. S.; Karpishin, T. B.; Novick, S. G.; Bierach, G.; O'Connell, J. F.; Westmoreland, T. D. *Inorg. Chem.* **1993**, *32*, 237.

(7) (a) Thorn, D. L. *Organometallics* **1982**, *1*, 197.

(8) For example, compound **1b** shows the formyl proton at 13.73 ppm in CD_3CN and **1a** showed this proton at 13.35 ppm.[3] The new isomer showed the formyl proton at 14.38 ppm: Gibson, D. H.; Andino, J. G. Unpublished observations.

(9) (a) Gibson, D. H.; Mandal, S. K.; Owens, K.; Richardson, J. F. *Organometallics* **1987**, *6*, 2624. (b) Gibson, D. H.; Owens, K. Mandal, S. K.; Sattich, W. E.; Franco, J. F. *Organometallics* **1991**, *10*, 1203. (c) Ellis, W. E.; Miedaner, A.; Curtis, C. J.; Gibson, D. H.; DuBois, D. L. *J. Am. Chem. Soc.* **2002**, *124*, 1926.

(10) Farrugia, L. J. *J. Appl. Crystallogr.* **1997**, *30*, 565.

(11) (a) Coe, B. J.; Glenwright, S. J. *Coord. Chem. Rev.* **2000**, *203*, 5. (b) Haukka, M.; Kiviaho, J.; Ahlgren, M.; Pakkanen, T. A. *Organometallics* **1995**, *14*, 825.

Table 1. Crystal Data and Structure Refinements

	2a	**3**	**4**	**2c**	**2b**
empirical formula	$C_{35}H_{31}F_6N_5O_2PRu$	$C_{20}H_{17}F_6N_4O_2PRu$	$C_{19}H_{20}F_6N_3O_2PRu$	$C_{28}H_{24}F_6N_5O_2PRu$	$C_{30.33}H_{24.66}Cl_{4.66}F_6N_5O_2PRu$
fw	753.12	591.42	584.42	708.56	899.96
temperature, K	100(2)	100(2)	100(2)	100(2)	100(2)
wavelength, Å	0.71073	0.71073	0.71073	0.71073	0.71073
cryst syst	triclinic	monoclinic	monoclinic	triclinic	triclinic
space group	$P\bar{1}$	$P2_1/c$	$C2/c$	$P\bar{1}$	$P\bar{1}$
unit cell dimens					
a, Å	8.8328(5)	8.631(4)	9.6583(11)	9.1217(14)	9.0418(11)
b, Å	13.8167(8)	12.916(6)	14.9249(11)	11.7259(18)	12.5923(15)
c, Å	14.0949(8)	20.429(10)	29.658(3)	13.791(12)	16.502(2)
α, deg	68.8830(10)	90	90	99.015(2)	98.148(2)
β, deg	73.4320(10)	91.110	95.428(2)	107.671(2)	102.492(2)
γ, deg	80.4520(10)	90	90	95.126(2)	94.394(2)
V, Å^3	1534.17(15)	2276.9(19)	4256.0(7)	1373.4(4)	1804.7(4)
Z	2	4	8	2	2
D(calcd), Mg/m^3	1.630	1.725	1.824	1.713	1.656
μ, mm^{-1}	0.639	0.833	0.892	0.708	0.892
F(000)	759	1176	2336	712	895
θ range, deg	1.84 to 28.21	1.87 to 27.88	1.38 to 27.98	1.58 to 28.11	1.64 to 28.00
no. reflns measd	13270	11533	18439	12193	10393
no. unique reflns (R_{int})	6879 (0.0176)	4725 (0.0503)	4932 (0.0260)	6159 (0.0367)	7373 (0.0176)
R1, wR2 ($I > 2\sigma(I)$)[a]	0.0350, 0.0898	0.0373, 0.0686	0.0292, 0.0646	0.0477, 0.1002	0.0511, 0.1074
R1, wR2 (all data)	0.0403, 0.0927	0.0584, 0.0711	0.0383, 0.0674	0.0707, 0.1070	0.0599, 0.1113
GOF	1.010	1.016	1.045	1.068	1.01
max diff peak, e Å^{-3}	0.820	0.848	0.690	1.120	0.936

[a] $R1 = \Sigma||F_o| - |F_c||/\Sigma|F_o|$; $wR2 = \{\Sigma[w(F_o^2 - F_c^2)^2]/\Sigma[w(F_o^2)^2]\}^{1/2}$.

Table 2. Selected Bond Distances (Å) and Bond Angles (deg) for 2a

Bond Distances			
C(1)−Ru	1.827(3)	N(3)−Ru	2.076(2)
C(2)−Ru	2.090(3)	N(4)−Ru	2.229(2)
N(1)−Ru	2.067(2)	C(1)−O(1)	1.158(3)
N(2)−Ru	2.135(2)		
Bond Angles			
Ru−C(1)−O(1)	177.3(3)	N(1)−Ru−N(2)	77.58(8)
C(1)−Ru−N(2)	173.26(10)	N(1)−Ru−N(3)	171.53(8)
C(2)−Ru−N(4)	166.52(11)	N(3)−Ru−N(4)	76.60(8)
C(1)−Ru−C(2)	88.77(13)		

Table 3. Selected Bond Distances (Å) and Angles (deg) for 3

Bond Distances			
C(1)−Ru	1.862(4)	N(4)−C(19)	1.152(4)
C(2)−Ru	2.102(3)	C(1)−O(1)	1.156(4)
N(1)−Ru	2.088(3)	C(2)−O(2)	1.431(4)
N(2)−Ru	2.027(3)	C(3)−O(2)	1.432(4)
N(3)−Ru	2.066(3)	C(19)−C(20)	1.456(5)
N(4)−Ru	2.155(3)		
Bond Angles			
C(1)−Ru−C(2)	91.84(14)	Ru−C(2)−O(2)	114.8(2)
C(1)−Ru−N(3)	100.93(13)	Ru−N(4)−C(19)	171.8(3)
C(1)−Ru−N2)	173.99(13)	N(2)−Ru−N(3)	78.78(12)
C(2)−Ru−N(4)	174.43(11)	N(1)−Ru−N(3)	157.27(12)
C(2)−O(2)−C(3)	111.8(2)	N(3)−Ru−N(4)	93.41(11)
Ru−C(1)−O(1)	177.7(3)	N(4)−C(19)−C(20)	178.3(4)

$\pi-\pi$ stacking.[12] Also, the angle between the ring normal between these two rings and the centroid is 21.12° and demonstrates their parallel displaced relationship. The pendant pyridine ring is also involved in intermolecular $\pi-\pi$ stacking with a pyridine ring in a bpy ligand. In this case the ring normal to centroid angle is 22.53°. Weaker intermolecular $\pi-\pi$ interactions, where the centroid distance is slightly more than 3.8 Å, appear to be present between coordinated pyridine rings of the terpyridine ligands; these also are of the parallel displaced type.

Efforts to convert formyl complex **1b** to the corresponding methoxymethyl complex by this method were unsuccessful; the acidic conditions were sufficient to convert it to the same metallacyclic complex that we recently reported from reaction of the hydroxymethyl complex with acid.[13] The structure of this metallacycle confirmed the stereochemistry that we had assigned to the hydroxymethyl complex and, by implication, the stereochemistry that was expected for formyl complex **1b**. Other known methods[9] for the synthesis of alkoxymethyl complexes were unsuccessful in generating complex **2b**. However, in probing the reactions of **2a** we were eventually led to a synthesis of this isomer, vide infra.

A sample of **2a** in acetonitrile was refluxed for 2 h, solvent was evaporated, and ^{1}H NMR analysis was performed. The analysis showed that most of **2a** had been consumed and that three new products were present, all of which appeared to contain methoxymethyl ligands. Also, the major product appeared to have lost the bpy ligand, but the other two retained it. A larger sample of **2a** was heated in the same way, and a purple product, whose spectral properties were the same as those of the major component generated in the first reaction, was isolated from the mixture. The product was purified and then identified as *cis*-[Ru(tpy)(CO)(MeCN)(CH_2OMe)]PF_6 (**3**); it was characterized by elemental analysis, ^{1}H and ^{13}C NMR and IR spectroscopy, and X-ray crystallography. The ORTEP diagram (cation only) is shown in Figure 2; crystallographic data are shown in Table 1. Selected bond distances and bond angles are shown in Table 3. As the diagram shows, the two carbon ligands remained cis to one another and the tpy ligand had become terdentate. The cation showed distorted octahedral geometry about the ruthenium atom as expected because of the fully chelated tpy ligand. The N(1)−Ru−N(3) bond angle involving the terminal pyridine nitrogens was severely distorted from linearity at 157.27(12)°. The ^{1}H NMR spectrum of **3** showed simple singlets for the methylene and methyl

(12) Janiak, C. *J. Chem. Soc., Dalton Trans.* **2000**, 3885
(13) Gibson, D. H.; Mashuta, M. S.; Andino, J. G. *Acta Crystallogr.* **2005**, *E61*, m341

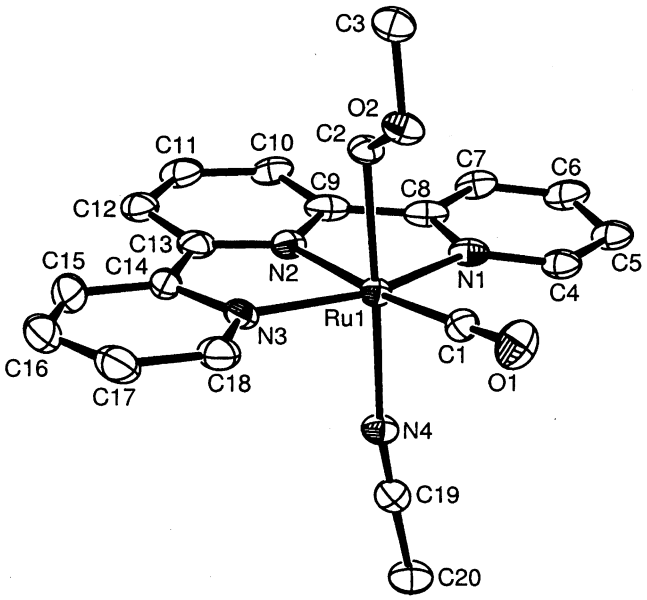

Figure 2. ORTEP drawing of **3** (cation only) with thermal ellipsoids shown at the 50% probability level.

protons of the methoxymethyl group at δ 3.52 and 2.70, respectively. In addition to the dissociative loss of the bpy ligand, it is clear that a structural change occurred in the conversion of **2a** to **3** since the middle terpyridine nitrogen is trans to the methoxymethyl group in **2a** but cis to it in **3**. We suggest that this transformation could occur as the result of complete displacement of the polypyridine ligands by MeCN during the reflux period to give *cis*-[Ru(MeCN)$_4$(CO)(CH$_2$OMe)]PF$_6$. Readdition of tpy, and loss of three solvent ligands, could have occurred during workup as the MeCN was evaporated; no intermediate complex was observed. Nondissociative ligand rearrangements of **2a**, such as those discussed below for **2b** and **2c**, will not yield an intermediate compound that could easily be converted to **3**.

It seemed likely that **3** was the precursor to at least one of the other two minor compounds generated from **2a**. Previously, we had successfully converted a structurally related complex, *cis*-[Ru(tpy)(CO)$_2$(MeCN)]2PF$_6$, to one containing bpy by displacing the solvent ligand and one of the terminal nitrogens of the tpy ligand.[3] We tried to do a similar conversion of **3**, with the expectation of creating an isomer of **2a**, but displacing the solvent ligand by bpy proved to be more difficult, and more complicated, than in the previous case. We then exchanged the acetonitrile ligand for MeOH in hopes that it would be more labile toward bpy than MeCN (see Experimental Section). The new green compound was identified as *cis*-[Ru(tpy)(CO)$_2$(MeOH)]2PF$_6$ (**4**) and was characterized by elemental analysis, ^{1}H and ^{13}C NMR and IR spectroscopy, and X-ray crystallography. The ORTEP diagram for **4** is shown in Figure 3, X-ray crystallographic data are shown in Table 1, and selected bond distances and bond angles are shown in Table 4. As in the case with **3**, the fully chelated tpy ligand led to distortion of the complex from regular octahedral geometry; the N(1)−Ru−N(3) bond angle was again severely distorted from linearity at 156.64(7)°.

Our initial efforts to convert **4** to an isomer of **2a** were complicated by the fact that heating **4** with bpy afforded three products rather than one. However, the ^{1}H NMR

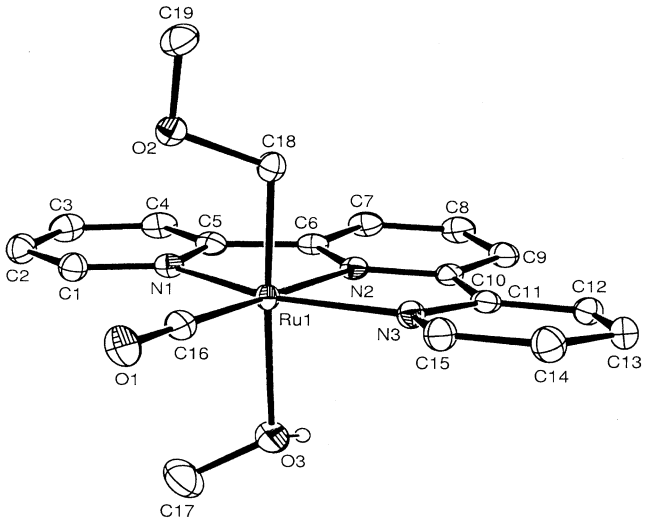

Figure 3. ORTEP drawing of **4** (cation only) with thermal ellipsoids shown at the 50% probability level.

Table 4. Selected Bond Distances (Å) and Bond Angles (deg) for 4

Bond Distances			
C(16)−Ru	1.858(2)	O(3)−Ru	2.3127(17)
C(18)−Ru	2.059(2)	C(16)−O(1)	1.154(3)
N(1)−Ru	2.0731(18)	C(17)−O(3)	1.426(3)
N(2)−Ru	2.0245(18)	C(18)−O(2)	1.439(3)
N(3)−Ru	2.0742(18)	C(19)−O(2)	1.422(3)

Bond Angles			
C(16)−Ru−C(18)	89.58(9)	C(18)−Ru−N(1)	90.57(8)
C(16)−Ru−N(1)	101.92(8)	C(18)−Ru−O(3)	176.93(7)
C(16)−Ru−N(2)	179.48(9)	C(18)−O(2)−C(19)	110.01(17)
C(16)−Ru−O(3)	92.70(8)	N(1)−Ru−N(2)	78.42(7)
C(17)−O(3)−Ru	119.17(16)	N(1)−Ru−N(3)	156.64(7)

Table 5. Selected Bond Distances (Å) and Bond Angles (deg) for 2c

Bond Distances			
C(1)−Ru	1.837(4)	N(3)−Ru	2.049(3)
C(2)−Ru	2.087(4)	N(4)−Ru	2.216(3)
N(1)−Ru	2.091(3)	C(1)−O(1)	1.140(4)
N(2)−Ru	2.173(3)	C(2)−O(2)	1.433(5)

Bond Angles			
Ru−C(1)−O(1)	176.9(3)	N(1)−Ru−N(2)	77.38(12)
Ru−C(2)−O(2)	116.0(2)	N(1)−Ru−N(3)	170.67(12)
C(1)−Ru−N(1)	85.99(14)	N(3)−Ru−N(4)	77.51(12)
C(1)−Ru−N(4)	164.81(14)	C(1)−Ru−C(2)	88.00(16)

spectral properties of two of these compounds were the same as those of the two unidentified products from heating **2a** in acetonitrile as discussed above. Milder conditions were needed, so we tried a procedure that had been used successfully to prepare a formaldehyde complex by ligand displacement.[14] Sonication of **4** together with bpy in CH_2Cl_2 at 0 °C afforded a single product, **2c**, an isomer of **2a**. It has been characterized by elemental analysis, ^{1}H and ^{13}C NMR and IR spectroscopy, and X-ray crystallography. The ORTEP diagram for **2c** (cation only) is shown in Figure 4, X-ray crystallographic data are shown in Table 1, and selected bond distances and bond angles are shown in Table 5. The distorted octahedral structure shows the bent C(1)−Ru−N(4) bond angle at 164.81(14)° and shows that the Ru−N bonds that are trans to the two carbon ligands are elongated relative to those that are trans to nitro-

(14) Gibson, D. H.; Franco, J. O.; Sleadd, B. A.; Naing, W.; Mashuta, M. S.; Richardson, J. F. *Organometallics* **1994**, *13*, 4570.

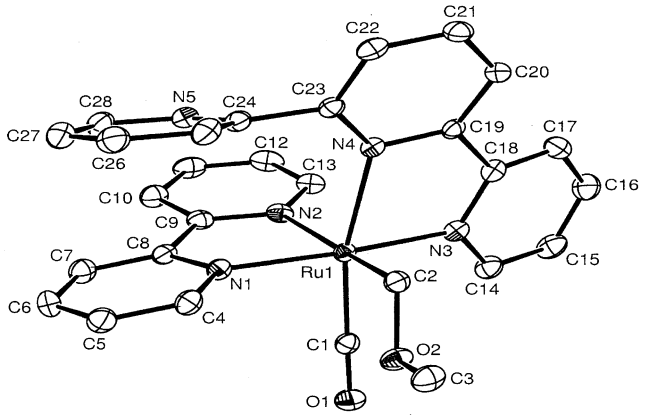

Figure 4. ORTEP drawing of **2c** (cation only) with thermal ellipsoids shown at the 50% probability level.

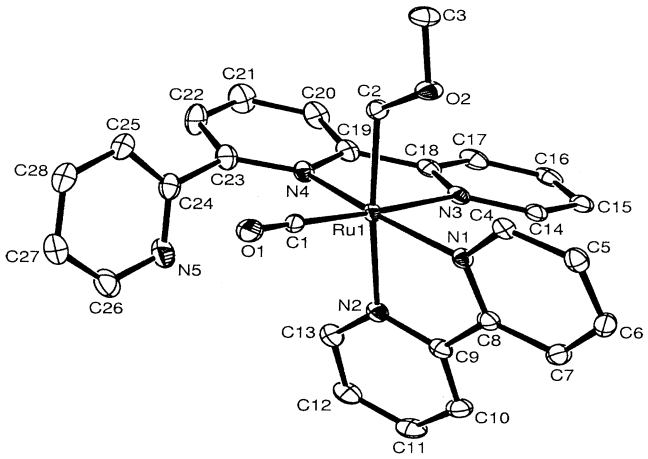

Figure 5. ORTEP drawing of **2b** (cation only) with thermal ellipsoids shown at the 50% probability level.

gen, a consequence of the trans influence of these ligands.[11] Compound **2c** has unique stereochemistry relative to the other compounds that we have prepared with bpy and tpy ligands (see Chart 1 and ref 3). As in the case of **2a**, the packing diagrams (see Figures 3a and 3b in the Supporting Information) for **2c** show intramolecular $\pi-\pi$ stacking between the pendant pyridine group and one of the pyridine groups of the bpy ligand (the offset angle is 23.08°) as well as intermolecular $\pi-\pi$ interactions between pendant pyridine groups (the offset angle is 21.50°; see Figures 2a and 2b in the Supporting Information). Weaker intermolecular interactions between bpy rings are also evident.

Analysis of ^{1}H NMR samples of **2c** that had been allowed to stand at room temperature showed that a second compound was being formed rapidly; the new compound had spectral properties that were identical with those of the third product from the reaction of **2a** in acetonitrile. The new product, **2b**, eventually became predominant in the mixtures, but the relative amount of **2b** to **2c** never became more than about 2:1. We tried to isolate the new compound from larger scale reactions of **2c** but were not successful. Also, reaction mixtures that were allowed to stand at room temperature for several hours began to develop small amounts of isomer **2a**. We needed a synthetic method that would enhance the amount of **2b** in the mixtures while minimizing **2a**. Using a 450 W mercury arc lamp placed in a water-cooled quartz immersion well, **2c** was irradiated in CD_2Cl_2 and maintained at room temperature. The best **2b** to **2c** ratio that we could obtain was about 2.7:1. Changing to dry, freshly distilled CH_2Cl_2 increased the ratio to 3.7:1. Compound **2a** degrades under irradiation, and neither it nor its degradation product created any separation problems in purifying **2b**. From this mixture, **2b** was isolated and fully characterized by elemental analysis, ^{1}H and ^{13}C NMR and IR spectroscopy, and X-ray crystallography. The ORTEP diagram for **2b** (cation only) is shown in Figure 5, X-ray crystallographic data are shown in Table 1, and selected bond distances and bond angles are shown in Table 6. As in the case of its isomers, **2b** showed distorted octahedral geometry about the ruthenium atom; the longest Ru−N bonds are the ones trans to the two carbon ligands, with the one trans to the methoxymethyl group being longest.[11] We examined the packing diagram for **2b** (see Figures 2a and 2b in the Supporting Information) and determined

Table 6. Selected Bond Distances (Å) and Bond Angles (deg) for 2b

	Bond Distances		
C(1)−Ru	1.824(4)	N(3)−Ru	2.136(3)
C(2)−Ru	2.115(4)	N(4)−Ru	2.106(3)
N(1)−Ru	2.081(4)	C(1)−O(1)	1.164(5)
N(2)−Ru	2.157(3)	C(2)−O(2)	1.439(5)
	Bond Angles		
Ru−C(1)−O(1)	172.4(4)	N(1)−Ru−N(2)	77.16(14)
Ru−C(2)−O(2)	116.5(3)	N(1)−Ru−N(4)	168.48(14)
C(1)−Ru−N(1)	89.18(16)	N(3)−Ru−N(4)	78.26(14)
C(1)−Ru−N(4)	102.16(16)	C(1)−Ru−C(2)	87.23(18)

that there are fewer $\pi-\pi$ stacking interactions for this isomer as compared to the other two and appear to involve mainly intermolecular interactions of the bpy ligands (offset angle is 21.93°), although some weaker intermolecular interactions involving the tpy ligands are also apparent. Compound **2b** is the linkage isomer of **2c** and has the stereochemistry assigned to formyl complex **1b** and the corresponding hydroxymethyl complex.[3]

During our efforts to isolate pure samples of **2b** from **2c**, it appeared that the two compounds were establishing equilibrium in solution. It was not clear whether a single isomer, or both of them, converted to **2a**, but the conversion generated an isomer of very different stereochemisty. Independent experiments were conducted with **2b** and **2c** to probe the linkage isomerization and the isomerization to **2a**. First, a sample of **2c** was placed in an NMR tube and dissolved in cold CD_2Cl_2 together with dimethyl oxalate as an internal standard and then placed in the NMR probe maintained at −5 °C; the ^{1}H NMR spectrum showed **2c** and the internal standard only. The probe temperature was then raised to 25 °C and spectra were recorded over several hours. The changes in composition of the sample are summarized in graphical form in Figure 6 (the full data are presented in the Supporting Information). As this figure indicates, the amount of **2c** dropped quickly during early stages of the experiment as **2b** was formed; **2a** was formed much more slowly. The same type of experiment was conducted with a sample of **2b**. The results are shown graphically in Figure 7 (full data are presented in the Supporting Information). The graphs do support the idea that **2b** and **2c** establish equilibrium since the ratio of the two isomers becomes approximately 2:1 fairly quickly from either starting material and remains at

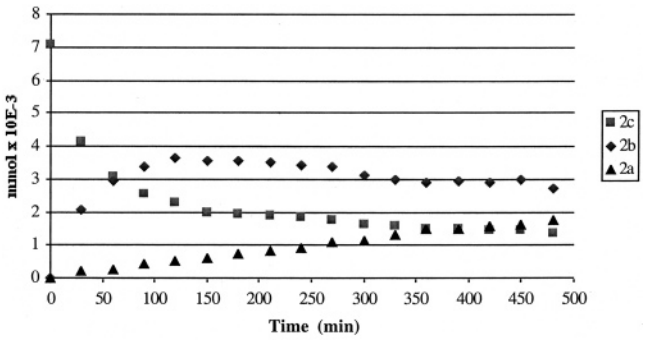

Figure 6. Graph of the isomerization of **2c** to **2b** and **2a**.

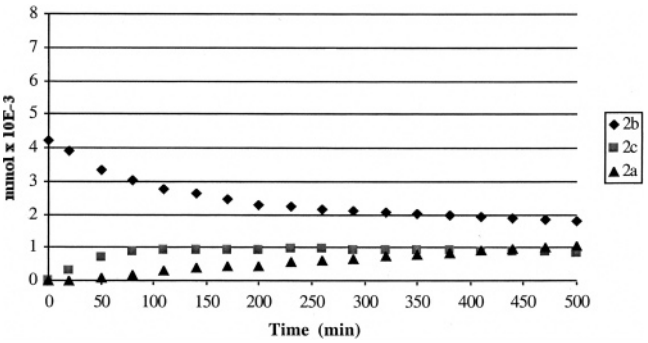

Figure 7. Graph of the isomerization of **2b** to **2c** and **2a**.

that value as the conversion to **2a** slowly occurs. Comparisons of the two graphs do not show a clear indication of which isomer is primarily responsible for the production of **2a**, although **2c** may have a slight edge. The isomerizations were conducted under very mild conditions, and in neither experiment was there any evidence for the dissociation of bpy or tpy; thus, the rearrangements are thought to be intramolecular.

There are several possible rearrangement pathways that have been considered for nondissociative reactions involving octahedral complexes.[15] One of these leads to a bicapped tetrahedral intermediate that is followed by rotation of two cis ligands. With the present compounds, this path seemed unlikely because of the severe steric crowding that would be present in the intermediate. Alternatively, the Bailar twist, or trigonal twist, path has been invoked to explain nondissociative polytopal rearrangements of a wide variety of compounds including those with chelating ligands.[16] Since our studies of the reactions of **2b**,**c** did not give clear preference to one versus the other in the isomerization to **2a**, possible trigonal twist paths have been considered for both of them. Scheme 2 shows examples of conversions of **2c** to **2a**, or to a linkage isomer of **2a** via trigonal twists; the linkage isomer has not been observed, but the steric interactions that are implied suggest that it should isomerize to **2a** readily. Scheme 3 shows examples of the conversion of **2b** to **2a**. Not all of the possible paths have been illustrated. Interestingly, the linkage isomerization that leads to the equilibration of **2b** and **2c** can be rationalized via a trigonal twist pathway also. The "tick-tock twist" mechanism has been established for

Scheme 2[a]

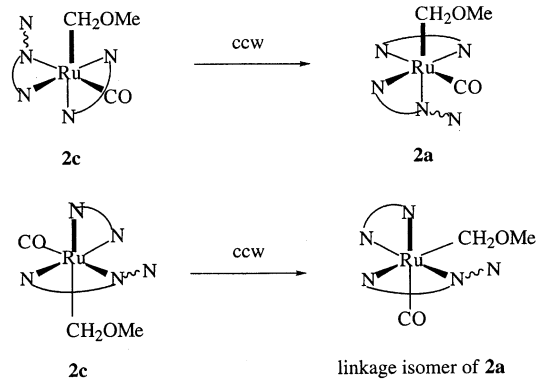

[a] N-N = 2,2′-bipyridine; N-N-N = 2,2′:6′,2″-terpyridine; bonds in bold fixed, others rotate counterclockwise.

Scheme 3[a]

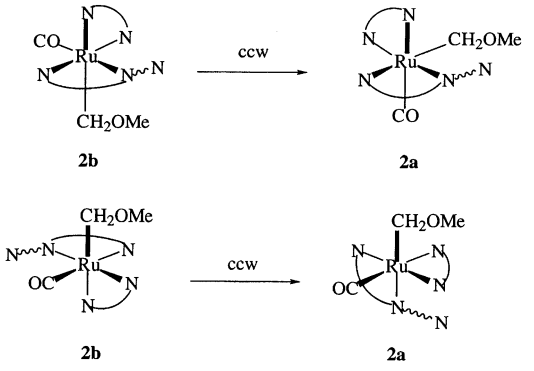

[a] N-N = 2,2′-bipyridine; N-N-N = 2,2:6′,2″-terpyridine; bonds in bold fixed, others rotate counterclockwise.

rearrangements, particularly linkage isomerizations, of some other compounds with η^2-tpy ligands.[17] We suggest a two-step, nondissociative pathway as a possible explanation for the transformation of **2b** to **2a**. The first step, the "conrotatory twist" path, would be initiated by reorganization of the chelated ligands and lead to the linkage isomer of **2a**; the second step would involve linkage isomerization only. The sequence is illustrated in Scheme 4.

Isomerizations of the type that we have observed for **2b** and **2c** are likely to be responsible for the isomerizations that were observed for **1b** and the corresponding hydroxymethyl complex as noted in the Introduction. In those cases, the minor isomers (presumably analogues of **2c**) are present in much lower concentration in solutions of the compounds than observed for the methoxymethyl complex.

Most of the trigonal twist variants for **2c** and the conrotatory twist for **2b** lead first to the linkage isomer of **2a** shown in Schemes 2 and 4. It was noted in the Introduction that this type of isomer would have the stereochemistry deemed necessary to promote migratory insertion. To this point, we have not observed any insertion products from reactions involving **2a**−**c**, nor have we observed methoxyacetic acid, the organic product expected from hydrolysis of the insertion product. Reactions of the compounds under electrochemical conditions, with and without CO_2, are being investigated.

(15) See: Ismail, A. A.; Sauriol, F.; Butler, I. S. *Inorg. Chem.* **1989**, *28*, 1007, and references therein.

(16) (a) Duffy, D. J.; Pignolet, L. H. *Inorg. Chem.* **1972**, *11*, 2843. (b) Eaton, S. S.; Eaton, G. R.; Holm, R. H.; Muetterties, E. L. *J. Am. Chem. Soc.* **1973**, *95*, 1116. (c) Lee, C. Y.; Wang, Y.; Liu, C. S. *Inorg. Chem.* **1991**, *30*, 3899.

(17) Gelling, A.; Orrell, K. G.; Osborne, A. G.; Sik, V. *J. Chem. Soc., Dalton Trans.* **1998**, 937.

Scheme 4[a]

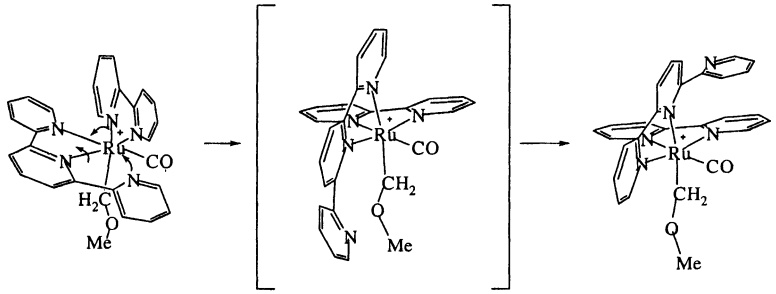

2b **2a**

[a] Conrotatory twist followed by linkage isomerization.

Experimental Section

General Procedures. Reagent grade solvents dichloromethane, acetone, acetonitrile, methanol, diethyl ether, toluene, and hexane (HPLC grade) were used as received except as noted. CD_3CN, tetrahydrofuran-d_8, and CD_2Cl_2 were obtained from Cambridge Isotope Laboratories. Chlorobenzene, NH_4PF_6, *p*-toluenesulfonic acid, CaH_2, and 2,2′-bipyridine were obtained from Aldrich and used as received. Compounds **1a** and **1b** were prepared according to the literature procedures.[3] Spectral data were obtained on the following instruments: NMR, Varian Unity Inova 500 MHz; FTIR, Mattson RS1; Gaussian peak deconvolution was accomplished with software for the Varian NMR.[18] Diffuse-reflectance data were obtained on the Mattson instrument with a DRIFTS accessory (Graseby Specac Inc.,"Mini-Diff") as KCl dispersions. ^1H and ^{13}C NMR spectra were referenced to residual protons in deuterated solvents. Sonication was done in a Bransonic ultrasonic cleaner (Fisher Scientific Co.). Melting points were obtained on a Thomas-Hoover capillary melting point apparatus and are uncorrected. Elemental analyses were performed by Midwest Microlab, Indianapolis, IN.

Synthesis of *cis,syn-N*-[Ru(bpy)(η^2-tpy)(CO)(CH_2OMe)]PF_6 (2a). *cis,syn*-N-[Ru(bpy)(η^2-tpy)(CO)(CHO)] PF_6 (**1a**; 1.67 g, 2.4 mmol) was placed in a three-necked 250 mL round-bottom flask and dissolved in 70 mL of CH_2Cl_2, which had been freshly distilled from CaH_2. The solution was placed in an ice bath and under a continuous flow of N_2. Then *p*-toluenesulfonic acid (0.45 g, 2.4 mmol) in 10 mL of CH_3OH, which had been freshly distilled from CaH_2, was placed in a dropping funnel, and the acid solution was added dropwise with stirring. After 30 min the ice bath was removed and the mixture stirred at room temperature for 30 min more. A white precipitate formed and the solution was deep red. The solution was again placed in an ice bath for 1 h. The mixture was then vacuum filtered and washed with 10 mL of saturated $NaHCO_3$ solution. The filtrate was then dried over $MgSO_4$, the mixture was filtered, and the filtrate was evaporated to dryness. The resulting residue was dissolved in 25 mL of CH_3CN. Saturated aqueous NH_4PF_6 (5 mL) was added and the solution evaporated until a red solid was suspended in the remaining solvent. The solid was collected by vacuum filtration and air-dried. The solid was dissolved in 25 mL of acetone, and then 15 mL of ether was added to precipitate the product, mp 114 °C. Yield: 0.76 g (88%). Anal. Calcd for $C_{28}H_{24}F_6N_5O_2PRu$: C, 47.46; H, 3.42. Found: C, 47.31; H, 3.40. IR (DRIFTS, KCl): ν_{CO} 1925 cm^{-1}. ^1H NMR (CD_3CN): δ 9.28 (d), 8.50 (d), 8.33 (d), 8.30 (d), 8.27 (t), 8.22 (d), 7.73 (t), 7.69 (t), 7.52 (d), 7.41 (d), 7.24 (m), 7.18 (dd), 6.95 (t), 3.91(d, IH, CH_2), 3.52 (d, 1H, CH_2), 3.02 (s, 3H, CH_3). ^{13}C NMR (CD_3CN): δ 205.00, 162.42, 159.36, 157.33, 156.06, 155.60, 155.07, 154.96, 150.47, 147.87, 140.04, 139.93, 139.70, 137.58, 136.27, 127.73, 126.68, 127.62, 127.36, 127.29, 126.05, 125.25, 124.50, 123.80, 123.75, 123.23, 76.28, 62.06.

Attempt to Synthesize Isomer 2b by the Method for 2a. *cis,syn*-C-[Ru(bpy)(η^2-tpy)(CO)(CHO)]·PF_6 (**1b**; 0.05 g, 0.07 mmol) was placed in a 25 mL Schlenk flask under N_2 and dissolved in 15 mL of CH_2Cl_2, which had been freshly distilled from CaH_2. The solution was placed in an ice bath. Then *p*-toluenesulfonic acid (0.013 g, 0.07 mmol) dissolved in 5 mL of CH_3OH, which had been freshly distilled from CaH_2, was placed in a dropping funnel, and the acid solution was added dropwise with stirring. The solution changed from yellow to red. After stirring for 1 h, the solvents were evaporated to dryness under vacuum. A ^1H NMR spectrum of the crude product taken in CD_3CN showed the previously characterized metallacycle[13] as the main product.

Efforts to Promote Isomerization of 2a. Compound **2a** (0.10 g, 0.14 mmol) was placed in a 100 mL round-bottom flask and dissolved in 50 mL of CH_3CN. After reflux for 2 h, the initial bright red solution became dark purple. A small sample (≈0.5 mL) was withdrawn from the mixture. The solution was evaporated to dryness and taken up in CD_3CN. ^1H NMR analysis showed that **2a** had been lost and another compound was the main component. Also, analysis of the methylene region indicated the presence of small amounts of two new compounds. The sample was allowed to stand at room temperature for 20 h and then examined with NMR, which showed that a small amount of **2a** had re-formed. The new compounds were still present.

Synthesis of *cis*-[Ru(tpy)(MeCN)(CO)(CH_2OMe)]PF_6 (3). Compound **2a** (0.30 g, 0.42 mmol) was placed in a 250 mL three-necked flask and dissolved in 100 mL of CH_3CN. The solution was refluxed for 2 h. After cooling, the solution was transferred into a 250 mL round-bottom flask along with 50 mL of toluene. The solvents were concentrated under vacuum with a rotary evaporator until about 5 mL of liquid remained. The liquid (colorless) was decanted and the solid residue was washed with 10 mL of hexane. The hexane was decanted and the residue was dried under vacuum. The residue was recrystallized from 15 mL of CH_3CN and 30 mL of toluene by slow evaporation under a N_2 constant flow. The product crystallized as deep red needles and was collected by vacuum filtration, mp 180 °C, dec. Yield: 0.19 g (75%). Anal. Calcd for $C_{20}H_{19}F_6N_4O_2PRu$: C, 40.48; H, 3.23; N, 9.44. Found: C, 40.82; H, 3.30; N, 9.25. IR (DRIFTS, KCl): ν_{CN} 2446, ν_{CO} 1934 cm^{-1}. ^1H NMR (CD_3CN): δ 8.72 (d), 8.30 (d), 8.24 (m), 8.00 (t), 7.45 (t), 3.52 (s, 2H, CH_2), 2.70 (s, 3H, CH_3), 1.96 (s, 3H, CH_3CN). ^{13}C NMR (CD_2Cl_2): δ 205.10, 156.63, 156.11, 155.15, 139.80, 138.07, 127.86, 123.99, 122.21, 119.66, 72.00, 61.26, 3.26.

Attempts to Prepare 2c from 3. (a) A sample of **3** (0.005 g, 8.4×10^{-3} mmol) in 0.5 mL of CD_2Cl_2 together with 2,2′-bipyridine (0.001 g, 8.4×10^{-3} mmol) was placed in an NMR tube and allowed to stand at 0 °C. After 3 days, analysis of the ^1H NMR spectrum showed that, even though the formation

(18) User Guide: Varian NMR Systems with VNMR 6.1B software, Varian Associates, Inc., 1998.

of **2a** had been inhibited, the combined amount of compounds **2b** and **2c** formed was roughly 30% of the total mixture.

(b) A sample of **3** (0.005 g, 8.4×10^{-3} mmol) in 1 g of CD_2Cl_2 together with excess 2,2′-bipyridine was heated at 45 °C for 5 min. Analysis by ^{1}H NMR showed that 15% of **1e** had already formed. The remainder consisted of a mixtue of **2b** and **2c**, with **2c** accounting for 50% of the whole mixture.

Synthesis of *cis*-[Ru(tpy)(MeOH)(CO)(CH$_2$OMe)]PF$_6$ (4). Compound **3** (0.10 g, 0.42 mmol) was placed in a 50 mL round-bottom flask and dissolved in 20 mL of CH_3OH. The mixture was stirred for 30 min, and then the green solution was evaporated to dryness. A fresh 10 mL of CH_3OH was added and the process repeated to ensure that the exchange of CH_3CN was complete. The solvent was evaporated to dryness, and the green residue was collected, mp 240 °C. Yield: 0.08 g (85%). Anal. Calcd for $C_{19}H_{20}F_6N_3O_3PRu$: C, 39.05; H, 3.45. Found: C, 38.89; H, 3.04. IR (DRIFTS, KCl): ν_{OH} 3129; ν_{CO} 1934 cm^{-1}. ^{1}H NMR (CD_3OD): δ 8.77 (d), 8.39 (d), 8.31 (d), 8.22 (t), 7.98 (t), 7.46 (t), 3.82 (s, 2H, CH_2), 3.27 (s, 3H, CH_3OH), 2.73 (s, 3H, CH_3). ^{13}C NMR (THF-d_8): δ 206.43, 158.12, 156.97, 156.59, 141.58, 139.38, 69.05, 68.10, 60.94.

Synthesis of 2c. Compound **4** (0.12 g, 0.18 mmol) was placed in a 100 mL Schlenk flask and dissolved in 50 mL of CH_2Cl_2. The solution was placed in an ice bath for 5 min. Then 2,2′-bipyridine (0.56 g, 3.6 mmol) was added, and the mixture was sonicated in an ice bath for 1 h. Then the solvent was removed under vacuum, and the residue was triturated with 25 mL of cold (4 °C) hexane. The suspended brown solid was separated by vacuum filtration and dissolved in 10 mL of cold CH_2Cl_2. Then 5 mL of cold hexane was added, and an orange solid precipitated and was collected by vacuum filtration, mp > 250 °C. Yield: 0.08 g (60%). Anal. Calcd for $C_{28}H_{24}F_6N_5O_2PRu$: C, 47.46; H, 3.42. Found: C, 47.48; H, 3.61. IR (DRIFTS, KCl): ν_{CO} 1943 cm^{-1}. ^{1}H NMR (CD_3CN): δ 9.12 (d), 8.61 (d), 8.41 (d), 8.20 (d), 8.11 (t), 8.06 (d), 7.99 (t), 7.79 (t), 7.66 (d), 7.55 (d), 7.44 (m), 7.33 (dd), 7.30 (t), 7.15 (d), 6.99 (d), 4.55 (d, 1H, CH_2), 4.19 (d, 1H, CH_2), 3.23 (s, 3H, CH_3). ^{13}C NMR (CD_3CN): δ 204.66, 162.13, 157.80, 156.72, 155.74, 155.45, 155.32, 155.27, 150.12, 149.74, 140.06, 139.52, 138.01, 137.67, 137.16, 128.76, 127.55, 127.43, 127.21, 126.84, 125.44, 125.00, 123.57, 123.48, 123.40, 75.73, 62.27.

Synthesis of *cis,syn-C*-[Ru(bpy)(η^2-tpy)(CO)(CH$_2$OMe)]PF$_6$ (2b). (a) Compound **2c** (0.05 g, 0.07 mmol) was dissolved in a 2.5 mL of CD_2Cl_2 and the solution divided into five NMR tubes. The tubes were placed radially around a 450 W UV lamp, which had been placed in a water-cooled quartz immersion thimble, at a distance of 26 cm; the temperature at the samples was 22 °C. The samples were irradiated with UV light for 2 h. Then they were transferred to a 50 mL round-bottom flask, and the solvent was evaporated to dryness. The residue was dissolved in a mixture of 2 mL of CH_2Cl_2 and 2 mL of chlorobenzene. Hexane (3 mL) was then added to the solution and the product precipitated from the solution at −30 °C. Yield: 0.01 g (24%). Anal. Calcd for $C_{28}H_{24}F_6N_5O_2PRu$: C, 47.46; H, 3.42. Found: C, 47.49; H, 3.70. IR (DRIFTS, KCl): ν_{CO} 1938 cm^{-1}. ^{1}H NMR (CD_3CN): δ 9.08 (d), 8.58 (d), 8.41 (br), 8.33 (d), 8.29 (dd), 8.21 (d), 8.11 (t), 8.00 (t), 7.92 (br), 7.65 (d), 7.58 (t), 7.44 (br), 7.38 (t), 7.30 (t), 7.18 (d), 3.87 (d, 1H, CH_2), 3.73 (d, 1H, CH_2), 3.11 (s, 3H, CH_3). ^{13}C NMR (CD_3CN): δ 200.63, 159.50, 157.86, 156.27, 155.23, 154.93, 154.84, 154.57, 154.11, 151.98, 149.73, 147.20, 138.91, 138.52, 138.36, 137.52, 136.96, 128.31, 127.07, 126.74, 124.83, 124.69, 123.60, 123.34, 123.02, 122.66, 73.84, 62.27.

(b) Compound **2c** (0.05 g, 0.07 mmol) was dissolved in a total of 5 mL of CH_2Cl_2, which had been freshly distilled from CaH_2, and placed in a 10 mm NMR tube. The sample was irradiated for 2 h using a 450 W UV lamp, which had been placed in a water-cooled quartz immersion thimble. After 2 h, a 0.5 mL sample was withdrawn from the tube and evaporated to dryness. The residue was taken up in CD_2Cl_2, and the ^{1}H NMR spectrum showed a mixture of compounds **2b** and **2c** in a ratio of 2.7 to 1, respectively. Compound **2a** was absent; it is known to degrade under these conditions.[19] The main sample was further irradiated for an additional 2 h, and another sample was removed for ^{1}H NMR analysis; the ratio of **2b** to **2c** had increased to 3.7:1. The main solution was transferred to a 10 mL round-bottom flask, hexane (3 mL) was added, and the solution was placed in a freezer at −30 °C. Compound **2b** was collected as red crystals.

Experiments to Monitor Isomerization. (a) Monitoring of a Sample of 2c. Under nitrogen, compound **2c** (0.005 g, 7×10^{-3} mmol) was placed in a septum-capped NMR tube immersed in an ice bath (0 °C) and then dissolved in 0.5 mL of cold CD_2Cl_2 injected through the septum. Then, 1 μL (3.4×10^{-5} g, 2.9×10^{-4} mmol) of a cold solution of dimethyl oxalate in CD_2Cl_2 (0.025 g in 1 g of CD_2Cl_2) was added with a syringe. The NMR probe's temperature was lowered to −5 °C, and the first spectrum was recorded. The first ^{1}H NMR spectrum confirmed that **2c** was the only isomer present; only the diasterotopic methylene protons for **2c**, at δ 4.27 and 4.54, appeared. The dimethyl oxalate showed a singlet at δ 3.88. Then the probe's temperature was raised to 25 °C and the time noted. ^{1}H NMR spectra of the sample were then obtained every 30 min. No color change was observed throughout the experiment, and the sample stayed as a deep red solution. Peak deconvolution[18] was necessary because of overlapping of the methylene resonances. Changes in isomer composition over time are plotted in Figure 6 (the data used to generate the graph are included in the Supporting Information).

After some time, a small amount of a reaction byproduct also appeared in the solution. Additional spectra were recorded intermittently until the conversion to **2a** was complete (≈4 days); the ratio of **2b** to **2c** stayed at approximately 2:1 until these isomers were consumed completely.

(b) Monitoring of a Sample of 2b. Compound **2b** (0.003 g, 5 μmol) was placed in a nitrogen-filled NMR tube immersed in an ice bath and dissolved in 0.5 mL of cold CD_2Cl_2 injected through a septum. As in experiment a, 1 μL (3.4×10^{-5} g, 2.9×10^{-4} mmol) of a cold solution of dimethyl oxalate in CD_2Cl_2 was added, by syringe, as an internal standard. The NMR probe's temperature was lowered to −5 °C, and the spectrum confirmed that the only components were **2b** and the internal standard. After this spectrum was recorded, the temperature of the probe was raised to 25 °C and the time recorded. Peak deconvolution[18] was necessary because of overlapping of the methylene resonances. Changes in the composition of the mixture over time are plotted in Figure 7 (the data used to generate the graph are included in the Supporting Information). After the solution had stood at room temperature for about 30 h, ^{1}H NMR analysis showed that compound **2a** had become the most abundant component of the mixture.

X-ray Crystallographic Studies. Compounds **2a**, **2b**, and **2c** exist as pairs of enantiomers; the ORTEP of only one enantiomer is shown in each case. All data were collected on a Bruker SMART APEX CCD diffractometer. The SMART software package[20] was used to acquire data. SAINT[21] was used to determine final cell parameters; absorption corrections were done using SADABS.[22] The structures were solved by direct methods using SHELXS-90[23] and refined by least-squares methods on F^2 using SHELXL-97[24] incorporated into

(19) Gibson, D. H.; Andino, J. G. Unpublished results

(20) *SMART*, version 5.628; Bruker Advanced X-ray Solutions, Inc.: Madison, WI, 2002.

(21) *SAINT*, version 6.36; Bruker Advanced X-ray Solutions, Inc.: Madison, WI, 2002.

(22) Sheldrick, G. M. *SADABS*, version 2.05; *Area Detector Absorption Correction*; University of Göttingen: Göttingen, Germany, 1997.

(23) Sheldrick, G. M. *SHELXS-90. Acta Crystallogr.* **1990**, *A46*, 467.

(24) Sheldrick, G. M. *SHELXL-97*, *Program for the Refinement of Crystal Structures*; University of Göttingen: Göttingen, Germany, 1997.

the SHELXTL suite of programs.[25] A more detailed text description of experimental crystallographic information is available in the Supporting Information.

An orange prism crystal of **2a** was mounted on a 0.05 mm CryoLoop with Paratone oil for collection of X-ray data at 100(2) K. Crystal data, data collection, and refinement parameters are listed in Table 1. The disorder in the methoxymethyl ligand was modeled using one two-thirds occupancy group (O2a and C3a) refined anisotropically and a second group (O2b and C3b) of one-third occupancy refined isotropically. A disordered toluene solvate is present and was modeled by using three full-occupancy ring carbons (C50−C52) and a half-occupancy methyl carbon (C53). The remaining atoms of the solvate are generated by symmetry (C50′−C53′). For all 6879 unique reflections (R_{int} = 0.0176) the final anisotropic full matrix least-squares refinement on F^2 for 436 variables converged at R1 = 0.040 and wR2 = 0.093 with a GOF of 1.01.

A thin orange plate of **2b**, mounted on a glass fiber, was used to collect X-ray data. The hexafluorophosphate anion was modeled with a "rocking" disorder using two six-atom groups of half-occupancy fluorine atoms (F1a−F6a and F1b−F6b), all refined anisotropically. The molecule contains two full-occupancy disordered methylene chloride and an additional one-third occupancy methylene chloride solvate. The first full-occupancy methylene chloride was modeled using a two-thirds and a one-third occupancy carbon atom (C80a and C80b, respectively) and three sets of one-third occupancy chloride atoms (Cl1a and Cl2a; Cl1b and Cl2b; Cl1c and Cl2c), in which all chlorides atoms were refined anisotropically. The second disordered methylene chloride solvate is modeled identically to the first using C90a, C90b, Cl3a, Cl3b, Cl3c Cl4a, Cl4b, and Cl4c. The partial occupancy solvate contains C70, Cl5, and Cl6 refined in the manner as described for the full-occupancy solvates. For all 7373 unique reflections (R(int) = 0.018) the final residuals based on F^2 for 541 variables are R1 = 0.059 and wR2 = 0.111 with a GOF of 1.01.

A red-orange prism of **2c**, mounted on a glass fiber, was used to collect X-ray data; crystallographic data are listed in Table 1. The hexafluorophosphate anion is modeled with a spinning top disorder using two four-atom groups of half-occupancy fluorine atoms (F3a−F6a and F3b−F6b) refined isotropically, in addition to the full-occupancy fluorines (F1 and F2). For all 6159 unique reflections (R(int) = 0.037) the final anisotropic full matrix least-squares refinement on F^2 for 469 variables converged at R1 = 0.048 and wR2 = 0.107 with a GOF of 1.07.

Structural determination on **3** was performed on a thin (0.25 × 0.20 × 0.01 mm^3) red-orange plate using a data acquisition strategy identical with that outlined above for **2a**. Crystal data are listed in Table 1. The disordered hexafluorophosphate anion was accurately modeled using two half-occupancy fluorine groups (F1a−F6a and F1b−F6b) octahedrally coordinated to a full-occupancy phosphorus atom, all refined anisotropically. For all 4725 unique reflections (R(int) = 0.049) the final anisotropic full matrix least-squares refinement on F^2 for 363 variables converged at R1 = 0.058 and wR2 = 0.071 with a GOF of 1.02.

A dark green prism of **4** mounted on a glass fiber was used for X-ray structural analysis via the data acquisition strategy identical with that described in the Supporting Information for **2a**. Crystallographic data are summarized in Table 1. The final residuals on F^2 for 359 variables converged at R1 = 0.038 and wR2 = 0.067 with a GOF of 1.04 for all 4932 data.

The files CCDC 27894−278598 (compounds **2a**, **2b**, **2c**, **3**, and **4**) contain the supplementary crystallographic data for this paper. These can be downloaded free of charge via www.ccdc.cam.ac.uk/conts/retrieving.hmtl (or from the Cambridge Crystallographic Data Centre, 12 Union Road, Cambridge, CB21EZ, U.K.; fax (+44) 1223-336-033; e-mail deposit@ccdc.cam.ac.uk).

Acknowledgment. This work was supported by the National Science Foundation (Grant No. 0203131). The CCD X-ray equipment was purchased through funds from the Kentucky Research Challenge Trust Fund. We thank Drs. Sudhir Ranjan and Chandi Pariya for preliminary work on some of these compounds.

Supporting Information Available: Tables giving full details of the crystallographic data and data collection parameters, atomic coordinates, anisotropic displacement parameters, bond distances, bond angles, and torsion angles for **2a**, **2b**, **2c**, **3**, and **4**. This material is available free of charge via the Internet at http://pubs.acs.org.

OM058031W

(25) *SHELXTL*, version 6.12, *Program Library for Structure Solution and Molecular Graphics*; Bruker Advanced X-ray Solutions, Inc.: Madison, WI, 2001.